Supporting Information

–

Investigating the Li^+ substructure and ionic transport in $Li_{10}GeP_{2-x}Sb_xS_{12}$ ($0 \leq x \leq 0.25$)

Bianca Helm,[a] Lara M. Gronych,[a] Ananya Banik,[a] Martin A. Lange,[a] Cheng Li,[b] and Wolfgang G. Zeier*[a,c]

[a]*Institute of Inorganic and Analytical Chemistry, University of Münster, Corrensstrasse 28/30, D-48149 Münster, Germany.*

[b]*Neutron Scattering Division, Oak Ridge National Laboratory (ORNL), 1 Bethel Valley Road, Oak Ridge, Tennessee 37831-6473, United States.*

[c]*Institut für Energie- und Klimaforschung (IEK), IEK-12: Helmholtz-Institut Münster, Forschungszentrum Jülich, 48149 Münster, Germany.*

**wzeier@uni-muenster.de*

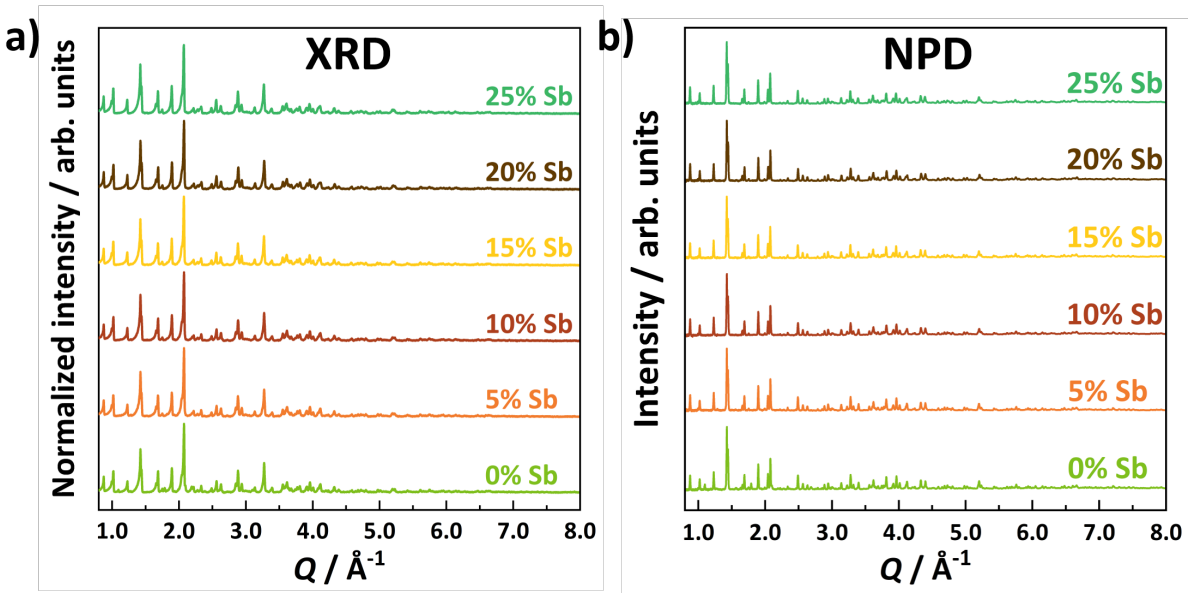

Figure S1: Display of (a) X-ray and (b) neutron diffraction data for the whole substitution series $Li_{10}GeP_{2-x}Sb_xS_{12}$ *(*$0 \leq x \leq 0.25$*).*

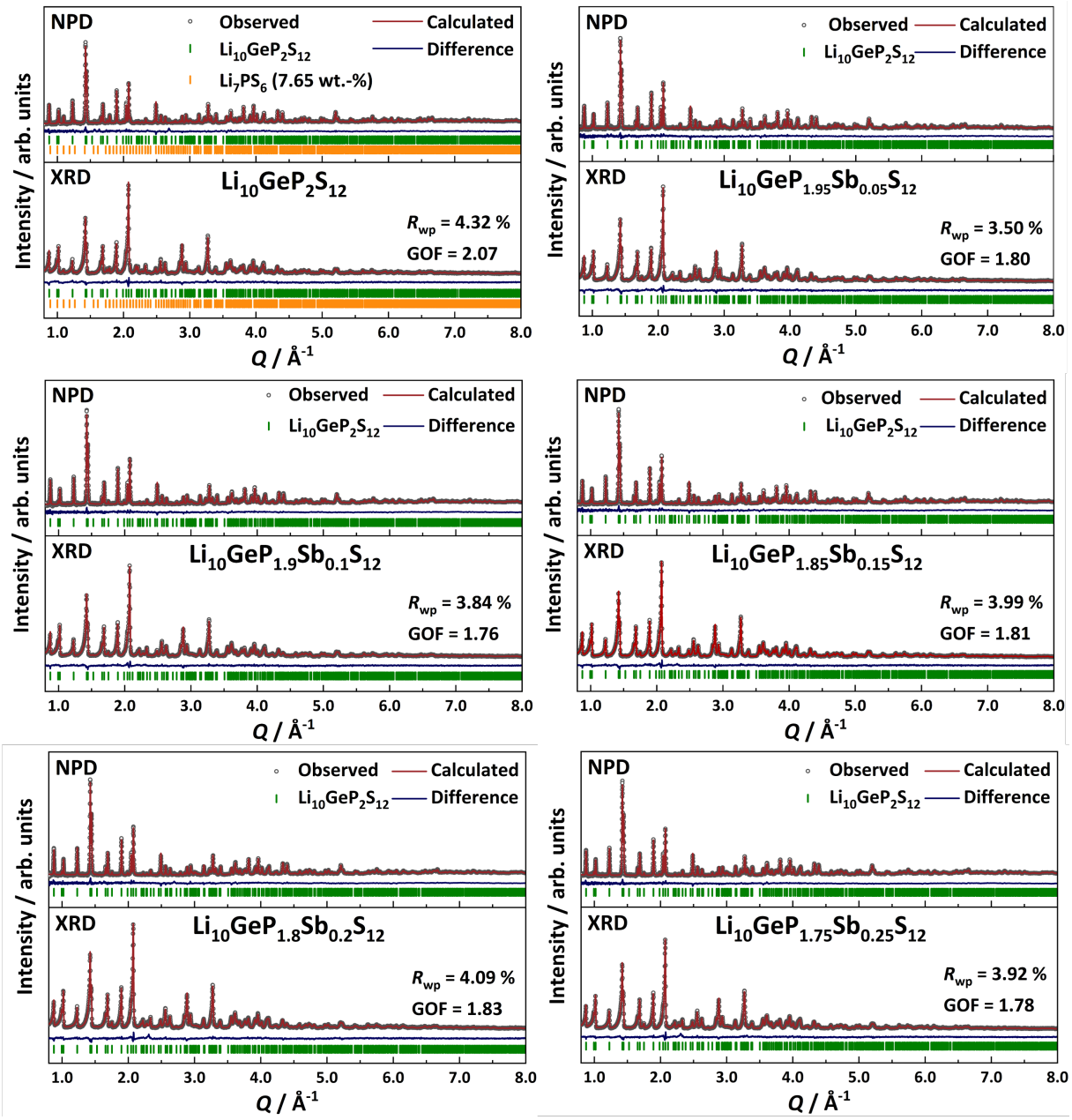

Figure S2: Rietveld refinements against neutron and X-ray diffraction data for the different substitution degrees in $Li_{10}GeP_{2-x}Sb_xS_{12}$. R_{wp} and GOF were used as an indicator for the fit quality. The d-spacings of the main phase ($Li_{10}GeP_2S_{12}$) as well as the side phase (Li_7PS_6) are displayed in different colors.

Table S1: Constraints used in the Rietveld refinements. Phosphorus, germanium and antimony occupy the same crystallographic site and the atomic coordinates and thermal displacement parameter were therefore constrained to the same value. Additionally, the lithium occupancy was constrained to nominal composition.

Atom	**Wyckoff position**	**Atomic coordinates**			***Occupancy***	B_{iso} / Å^2
		x	***y***	***z***		
Li(1)	16*h*	Pos1	Pos2	Pos3	(20 – Occ1·4 – Occ2·16 – Occ3·4)/16	Th1
Li(2)	4*d*	0.25	0.25	Pos4	Occ1	Th2
Li(3)	16*h*	Pos5	Pos6	Pos7	Occ2	Th3
Li(4)	4*c*	0.25	0.75	Pos8	Occ3	Th4
P(1)	4*d*	0.25	0.25	Pos9	0.5 – Occ4	Th5
Sb(1)	4*d*	0.25	0.25	Pos9	Occ4	Th5
Ge(1)	4*d*	0.25	0.25	Pos9	0.5	Th5
P(2)	2*b*	0.25	0.25	0.75	1	Th6
S(1)	8*g*	0.25	Pos10	Pos11	1	Th7
S(2)	8*g*	0.25	Pos12	Pos13	1	Th8
S(3)	8*g*	0.25	Pos14	Pos15	1	Th9

Table S2: Structural data for the nominal composition $Li_{10}GeP_2S_{12}$ at 300 K.

$Li_{10}GeP_2S_{12}$ ***Lattice parameter: a = b = 8.7093(1) Å, c = 12.6168(2) Å*** ***R_{wp} = 4.32 %, GOF = 2.07, space group = $P4_2/nmc$ (No. 137, origin 2)***						
Atom	Wyckoff position	Atomic coordinates			*Occ.*	B_{iso} / Å^2
		x	***y***	***z***		
Li(1)	16*h*	0.498(1)	0.015(1)	0.4415(6)	0.490(8)	6.0(3)
Li(2)	4*d*	0.25	0.25	0.1956(6)	0.94(1)	3.1(2)
Li(3)	16*h*	0.515(1)	−0.018(1)	0.2854(7)	0.344(7)	3.2(3)
Li(4)	4*c*	0.25	0.75	0.498(1)	0.72(1)	6.6(5)
P(1)	4*d*	0.25	0.25	0.9417(3)	0.5	1.26(3)
Ge(1)	4*d*	0.25	0.25	0.9417(3)	0.5	1.26(3)
P(2)	2*b*	0.25	0.25	0.75	1	1.40(5)
S(1)	8*g*	0.25	0.9389(2)	0.6578(2)	1	2.30(5)
S(2)	8*g*	0.25	0.0462(2)	0.3473(2)	1	1.83(5)
S(3)	8*g*	0.25	0.4490(2)	0.0415(2)	1	1.76(5)

Table S3: Structural data for the nominal composition $Li_{10}GeP_{1.95}Sb_{0.05}S_{12}$ at 300 K.

$Li_{10}GeP_{1.95}Sb_{0.05}S_{12}$ ***Lattice parameter: a = b = 8.7114(2) Å, c = 12.6171(3) Å*** ***R_{wp} = 3.50 %, GOF = 1.80, space group = $P4_2/nmc$ (No. 137, origin 2)***						
Atom	Wyckoff position	Atomic coordinates			*Occ.*	B_{iso} / Å^2
		x	***y***	***z***		
Li(1)	16*h*	0.499(1)	0.017(1)	0.4387(6)	0.477(8)	5.1(3)
Li(2)	4*d*	0.25	0.25	0.1955(6)	0.93(1)	3.4(2)
Li(3)	16*h*	0.514(1)	−0.020(1)	0.2870(7)	0.358(7)	4.1(3)
Li(4)	4*c*	0.25	0.75	0.498(1)	0.72(1)	7.3(5)
P(1)	4*d*	0.25	0.25	0.9411(1)	0.477(2)	1.47(3)
Sb(1)	4*d*	0.25	0.25	0.9411(1)	0.022(2)	1.47(3)
Ge(1)	4*d*	0.25	0.25	0.9411(1)	0.5	1.47(3)
P(2)	2*b*	0.25	0.25	0.75	1	1.44(5)
S(1)	8*g*	0.25	0.9386(2)	0.6581(2)	1	2.21(5)
S(2)	8*g*	0.25	0.0462(2)	0.3478(2)	1	1.71(5)
S(3)	8*g*	0.25	0.4488(2)	0.04093(2)	1	1.58(5)

Table S4: Structural data for the nominal composition $Li_{10}GeP_{1.9}Sb_{0.1}S_{12}$ at 300 K.

$Li_{10}GeP_{1.9}Sb_{0.1}S_{12}$ ***Lattice parameter: a = b = 8.7063(2) Å, c = 12.6233(3) Å*** ***R_{wp} = 3.84 %, GOF = 1.76, space group = $P4_2/nmc$ (No. 137, origin 2)***						
Atom	Wyckoff position	Atomic coordinates			*Occ.*	B_{iso} / Å^2
		x	***y***	***z***		
Li(1)	16*h*	0.499(1)	0.017(1)	0.4399(6)	0.484(8)	5.8(3)
Li(2)	4*d*	0.25	0.25	0.1959(6)	0.92(1)	3.5(2)
Li(3)	16*h*	0.514(1)	−0.021(1)	0.2866(7)	0.357(6)	4.1(3)
Li(4)	4*c*	0.25	0.75	0.498(1)	0.71(1)	7.0(5)
P(1)	4*d*	0.25	0.25	0.9409(1)	0.453(2)	1.52(3)
Sb(1)	4*d*	0.25	0.25	0.9409(1)	0.046(2)	1.52(3)
Ge(1)	4*d*	0.25	0.25	0.9409(1)	0.5	1.52(3)
P(2)	2*b*	0.25	0.25	0.75	1	1.51(5)
S(1)	8*g*	0.25	0.9381(2)	0.6582(2)	1	2.26(5)
S(2)	8*g*	0.25	0.0451(2)	0.3472(2)	1	1.75(5)
S(3)	8*g*	0.25	0.4493(2)	0.0411(2)	1	1.62(5)

Table S5: Structural data for the nominal composition $Li_{10}GeP_{1.85}Sb_{0.15}S_{12}$ at 300 K.

$Li_{10}GeP_{1.85}Sb_{0.15}S_{12}$ ***Lattice parameter: a = b = 8.7135(2) Å, c = 12.6384(3) Å*** ***R_{wp} = 3.99 %, GOF = 1.81, space group = $P4_2/nmc$ (No. 137, origin 2)***						
Atom	Wyckoff position	Atomic coordinates			*Occ.*	B_{iso} / Å^2
		x	***y***	***z***		
Li(1)	16*h*	0.5005(9)	0.018(1)	0.4390(5)	0.470(8)	5.1(2)
Li(2)	4*d*	0.25	0.25	0.1958(6)	0.94(1)	3.6(2)
Li(3)	16*h*	0.515(1)	−0.022(1)	0.2874(7)	0.366(6)	4.4(3)
Li(4)	4*c*	0.25	0.75	0.5002(11)	0.71(1)	7.4(5)
P(1)	4*d*	0.25	0.25	0.9409(1)	0.437(2)	1.48(3)
Sb(1)	4*d*	0.25	0.25	0.9409(1)	0.062(2)	1.48(3)
Ge(1)	4*d*	0.25	0.25	0.9409(1)	0.5	1.48(3)
P(2)	2*b*	0.25	0.25	0.75	1	1.28(5)
S(1)	8*g*	0.25	0.9384(2)	0.6578(2)	1	2.19 (5)
S(2)	8*g*	0.25	0.0448(2)	0.3469(2)	1	1.82(5)
S(3)	8*g*	0.25	0.4494(2)	0.0410(2)	1	1.67(5)

Table S6: Structural data for the nominal composition $Li_{10}GeP_{1.8}Sb_{0.2}S_{12}$ at 300 K.

$Li_{10}GeP_{1.8}Sb_{0.2}S_{12}$ ***Lattice parameter: a = b = 8.6989(2) Å, c = 12.6361(3) Å*** ***R_{wp} = 4.09 %, GOF = 1.83, space group = $P4_2/nmc$ (No. 137, origin 2)***						
Atom	Wyckoff position	Atomic coordinates			*Occ.*	B_{iso} / Å^2
		x	***y***	***z***		
Li(1)	16*h*	0.497(1)	0.016(1)	0.4406(6)	0.483(8)	6.2(3)
Li(2)	4*d*	0.25	0.25	0.1954(6)	0.92(1)	3.9(2)
Li(3)	16*h*	0.516(1)	−0.024(1)	0.2862(7)	0.360(6)	4.3(3)
Li(4)	4*c*	0.25	0.75	0.499(1)	0.70(1)	6.6(5)
P(1)	4*d*	0.25	0.25	0.9409(1)	0.416(2)	1.55(3)
Sb(1)	4*d*	0.25	0.25	0.9409(1)	0.083(2)	1.55(3)
Ge(1)	4*d*	0.25	0.25	0.9409(1)	0.5	1.55(3)
P(2)	2*b*	0.25	0.25	0.75	1	1.43(5)
S(1)	8*g*	0.25	0.9373(2)	0.6582(2)	1	2.28 (5)
S(2)	8*g*	0.25	0.0432(2)	0.3466(2)	1	1.84(5)
S(3)	8*g*	0.25	0.4496(2)	0.0413(2)	1	1.73(5)

Table S7: Structural data for the nominal composition $Li_{10}GeP_{1.75}Sb_{0.25}S_{12}$ at 300 K.

$Li_{10}GeP_{1.75}Sb_{0.25}S_{12}$ ***Lattice parameter: a = b = 8.7133(2) Å, c = 12.6515(3) Å*** ***R_{wp} = 3.92 %, GOF = 1.78, space group = $P4_2/nmc$ (No. 137, origin 2)***						
Atom	Wyckoff position	Atomic coordinates			*Occ.*	B_{iso} / Å^2
		x	***y***	***z***		
Li(1)	16*h*	0.502(1)	0.017(1)	0.4380(6)	0.472(8)	5.2(2)
Li(2)	4*d*	0.25	0.25	0.1949(6)	0.92(1)	3.5(2)
Li(3)	16*h*	0.513(1)	−0.024(1)	0.2885(7)	0.367(6)	4.6(3)
Li(4)	4*c*	0.25	0.75	0.499(1)	0.72(1)	7.6(5)
P(1)	4*d*	0.25	0.25	0.9409(1)	0.408(2)	1.43(3)
Sb(1)	4*d*	0.25	0.25	0.9409(1)	0.092(2)	1.43(3)
Ge(1)	4*d*	0.25	0.25	0.9409(1)	0.5	1.43(3)
P(2)	2*b*	0.25	0.25	0.75	1	1.19(5)
S(1)	8*g*	0.25	0.9378(2)	0.6576(2)	1	2.19 (5)
S(2)	8*g*	0.25	0.0437(2)	0.3463(2)	1	1.86(5)
S(3)	8*g*	0.25	0.4495(2)	0.0411(2)	1	1.64(5)

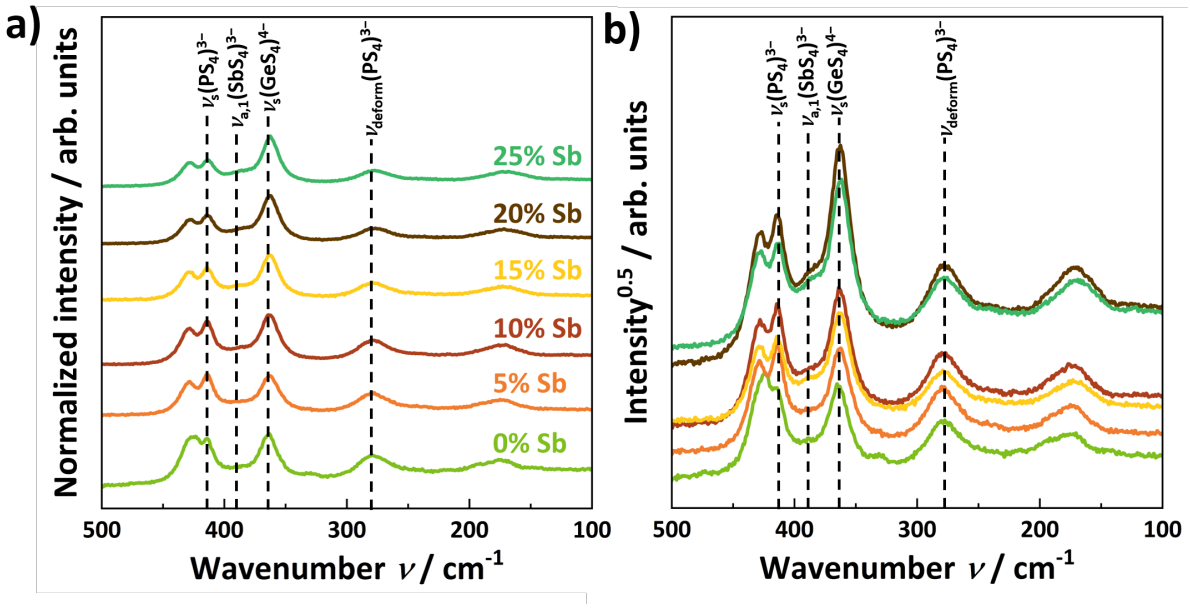

Figure S3: (a) Display of Raman spectra of the different samples showing a similar pattern. (b) Square root plot of the Raman spectra to emphasize the development of a shoulder at 387 cm^{-1}. The symmetric (ν_s) and deformation (ν_{deform}) stretch of the $(PS_4)^{3-}$ unit, the symmetric stretch of the $(GeS_4)^{4-}$ unit and the asymmetric ($\nu_{a,1}$) stretch of the $(SbS_4)^{3-}$ unit were observed.[1–3]

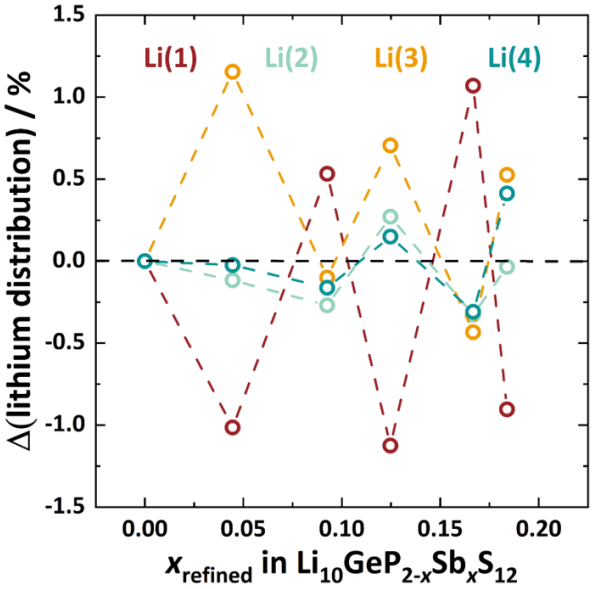

Figure S4: Change in Li^+ occupancy per substitution step relative to the previous substitution step indicating that around 1% of Li^+ ions are shifted between the lithium positions.

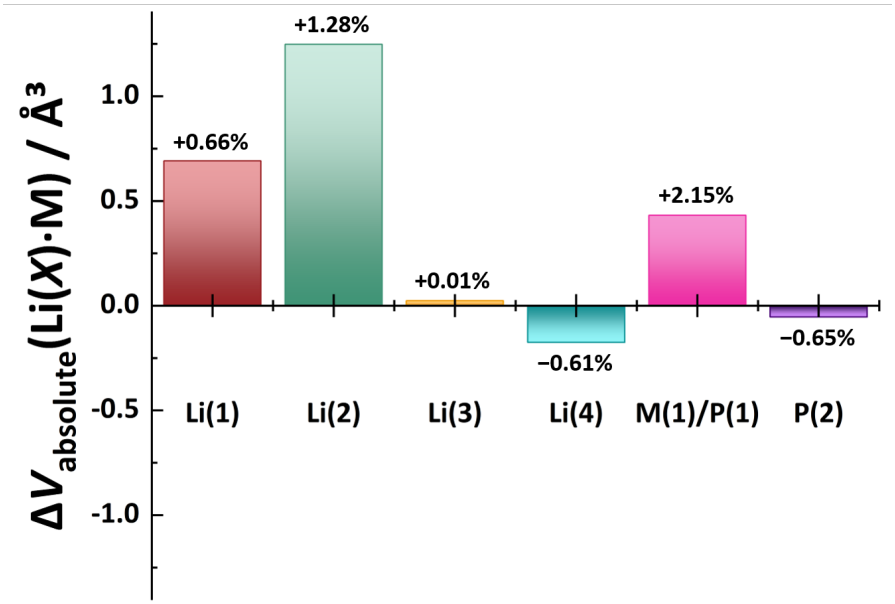

Figure S5: Relative change in polyhedral volume of each respective crystallographic site and the absolute change of polyhedral volume for all Li(X) polyhedra in the unit cell. The relative change was calculated by subtracting the volumes of $x_{nom}(Sb) = 0$ from 0.25 and dividing by the volume of $x_{nom}(Sb) = 0.25$. The absolute change was determined by subtracting the volume of $x_{nom}(Sb) = 0$ from 0.25, subsequently multiplying with the respective multiplicity M of each site were used.

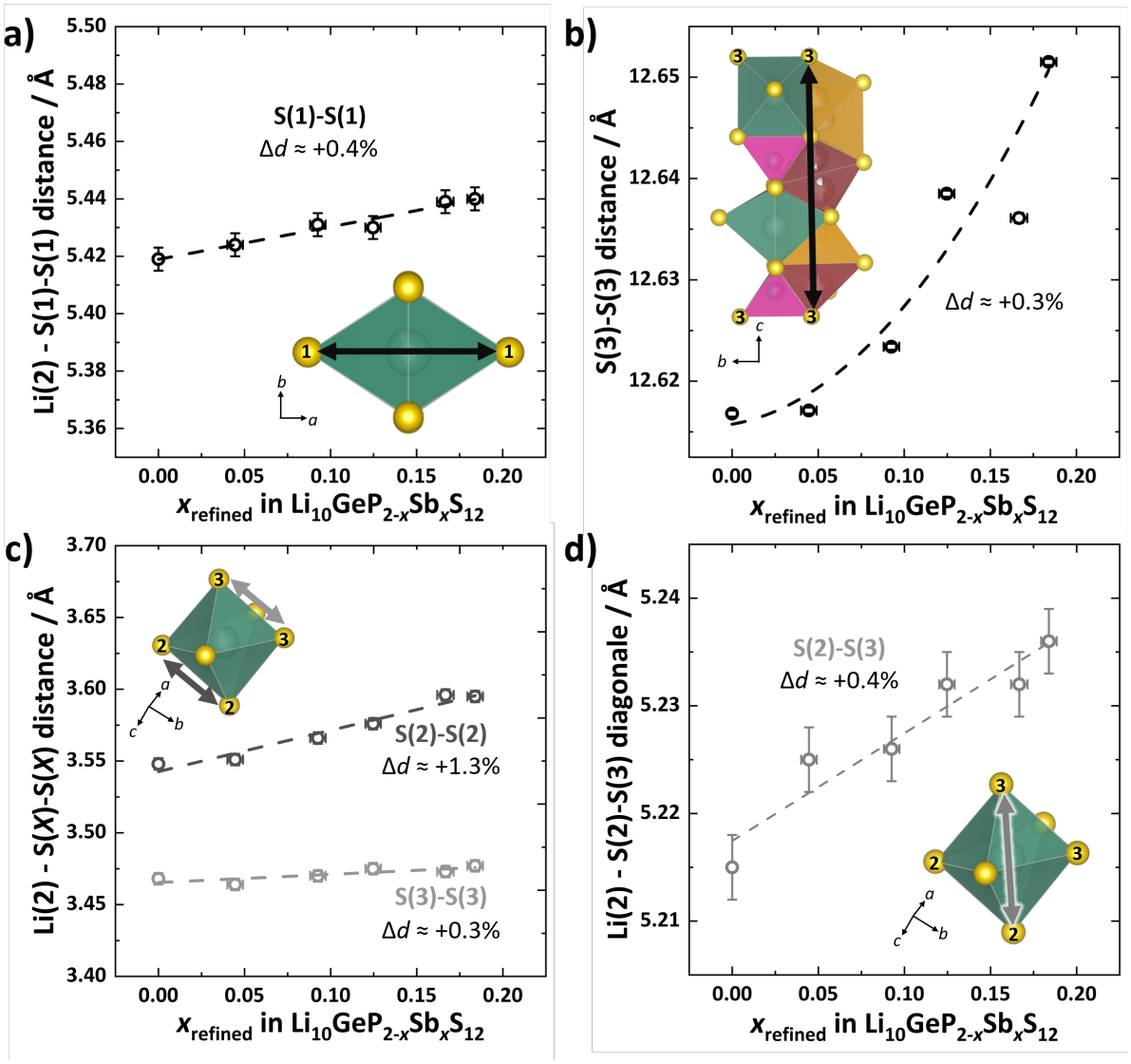

Figure S6: (a) The S(1)-S(1) distance in the Li(2) octahedron is increasing showing an expansion into the ab-plane. (b)The S(3)-S(3) distance increases with higher antimony content. The inset shows that the Li(1)-Li(3) chain and Li(2)-M(1)/P(1) chain are connected via S(3) which suggests a similar expansion in c-direction. (c) The S(2)-S(2) distances increases, while the S(3)-S(3) distance remains similar. Both S(X)-S(X) arrangements are located in the ab-plane. (d) The diagonal of S(2)-S(3) square is increasing which is indicative for an increase in c-direction. The dashed lines are added as guides-to-the-eyes and all structural changes are giving in percentage to gauge the minor overall changes.

Table S9: Height and relative density of the pellets used for temperature-dependent impedance measurements in pouch cells.

x_{nom} in $Li_{10}GeP_{2-x}Sb_xS_4$	pellet height / cm	relative pellet density / %
0	0.196	74
0.05	0.194	80
0.10	0.192	75
0.15	0.192	75
0.20	0.178	74
0.25	0.184	74

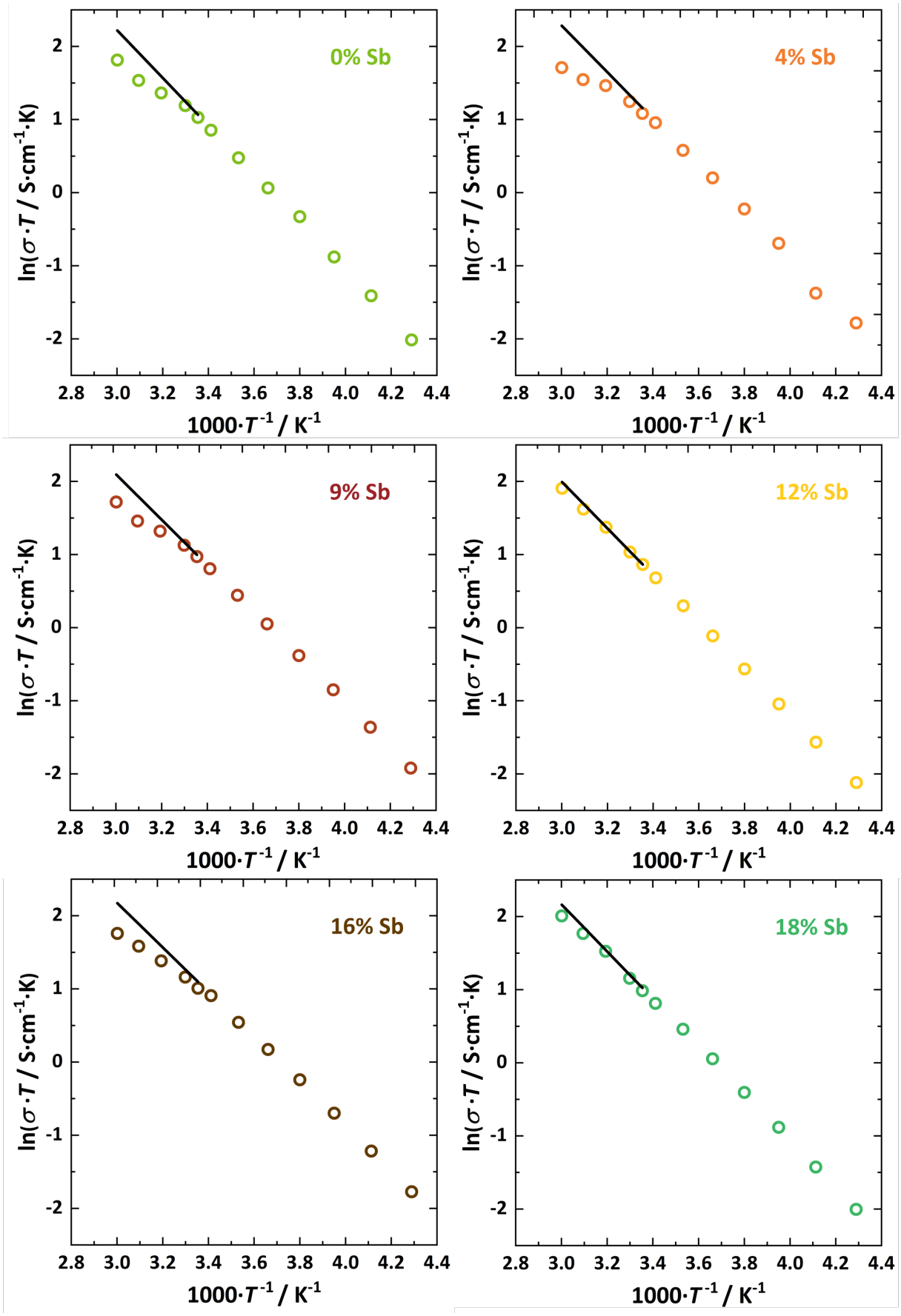

Figure S7: Display of the Arrhenius plots of the substitution series from −40°C up to 60°C showing that at higher temperatures the determined conductivity is underestimated to a certain

extent due to the occurring inductance. The underestimation is lesser or stronger depending on the sample (○ = measured data; straight line = extrapolated data).

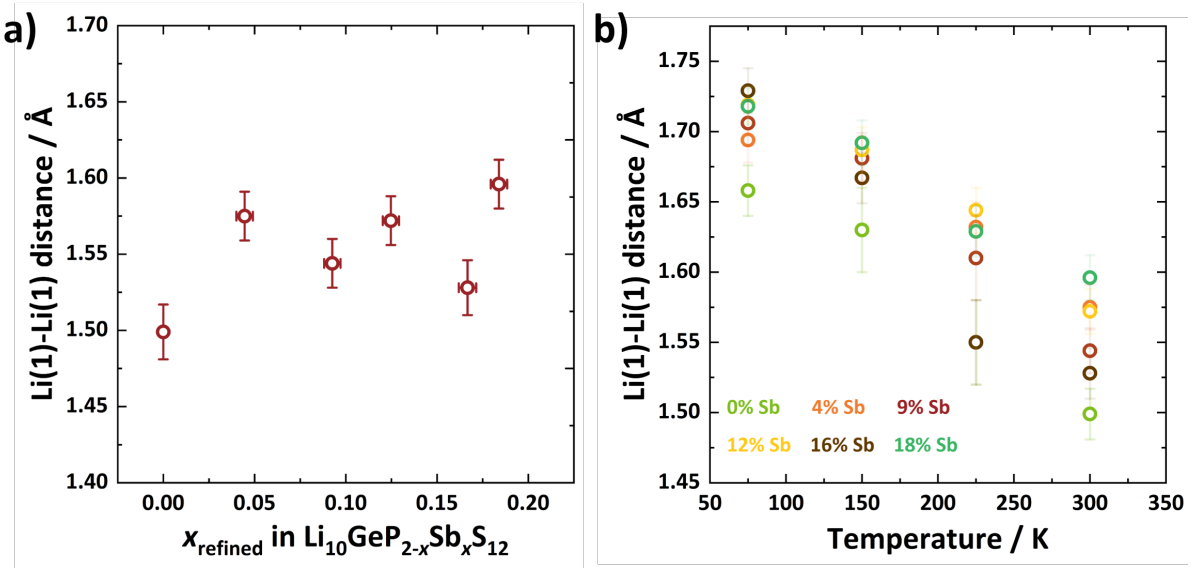

Figure S8: (a) The change in Li(1)-Li(1) distance dependent on the Sb content in LGPS. (b) Temperature-dependent behavior of the Li(1)-Li(1) distance.

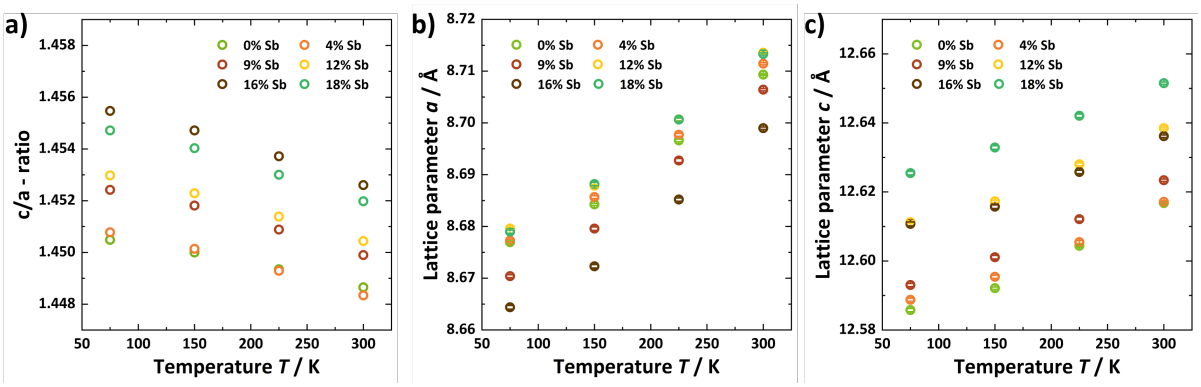

Figure S9: Illustration of temperature dependence on (a) the c/a-ratio, (b) lattice parameter a and (c) lattice parameter of $Li_{10}GeP_{2-x}Sb_xS_{12}$.

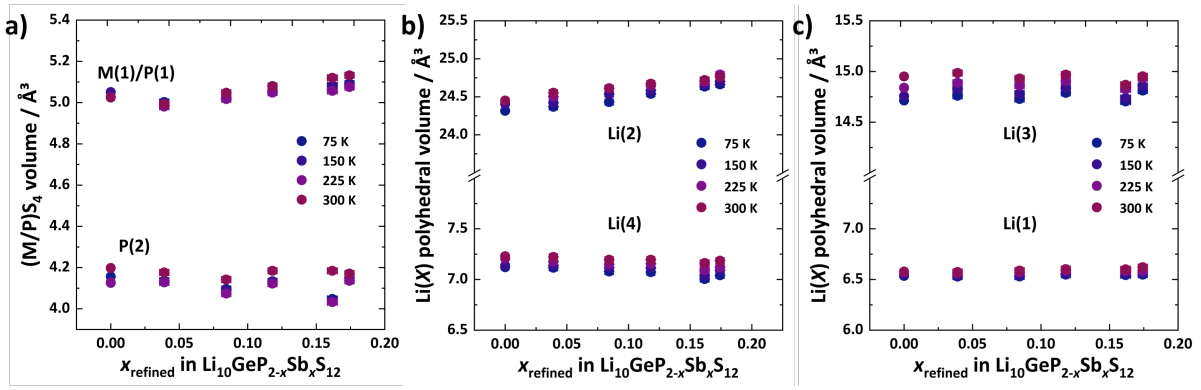

Figure S10: The volume changes of (a) M(1)/P(1) and P(2), (b) Li(2) and Li(4) as well as (c) Li(1) an d Li(3) are shown.

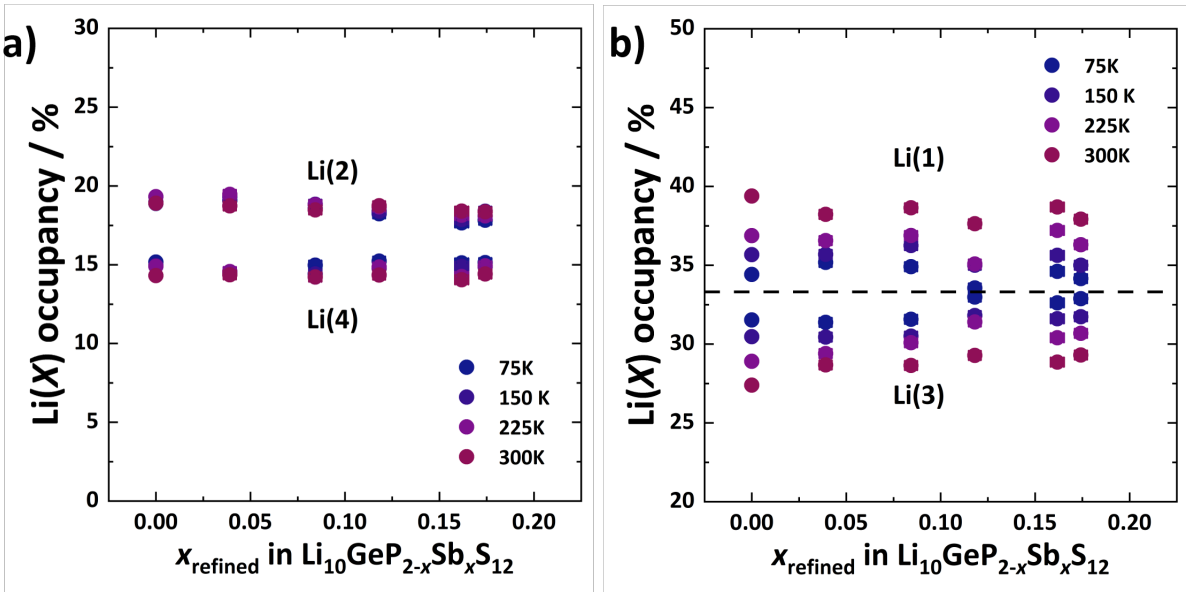

Figure S11: Lithium distribution dependent on the temperature showing that (a) Li(2) and Li(4) occupancy is similar for all temperatures, while (b) for Li(1) and Li(3) the Li^+ ions redistribute with temperature. Lower temperatures have comparable occupancies for Li(1) and Li(3), while at higher temperatures Li(1) is preferably occupied. The dashed line in (b) is for clarifying the different data sets.

References

1 W. Mikenda and A. Preisinger, *Spectrochim. Acta Part A Mol. Spectrosc.*, 1980, **36**, 365–370.

2 T. Fuchs, S. P. Culver, P. Till and W. G. Zeier, *ACS Energy Lett.*, 2020, **5**, 146–151.

3 S. P. Culver, A. G. Squires, N. Minafra, C. W. F. Armstrong, T. Krauskopf, F. Böcher, C. Li, B. J. Morgan and W. G. Zeier, *J. Am. Chem. Soc.*, 2020, **142**, 21210–21219.